Development of Microwave Imaging System for Stroke Detection

(Pembangunan Sistem Pengimejan Gelombang Mikro bagi Pengesahan Strok)

*Chow Kah Wei, Norbahiah Misran and Mohammad Tariqul Islam
Department of Electrical, Electronics and Systems Engineering
Faculty of Engineering & Built Environment, Universiti Kebangsaan Malaysia
**Corresponding author: chowkahwei1996@hotmail.com*

ABSTRACT

Dating back to 2400 years ago, stroke had been constantly plagued the society regardless. With the advancement of technology, machines like the computerized tomography (CT) and magnetic resonance imaging (MRI) machines still can't provide on the move diagnosis. Due to their bulky size and coupled that with dangerous radiation emitted by CT machines, ambulance will no longer be conducive and safe for transporting patients if it is installed into it. An expensive and high operating cost means that majority of the population just can't afford. Therefore, this is where microwave imaging technology will help solve. Microwave imaging technology is capable of penetrating inside dielectric materials while being relatively small and portable. Thus, the main aims of this project are to analyses an existing system, design and develop a prototype and validate the system. A microwave imaging system for stroke detection is presented. It is consisted of a rotating platform powered by Arduino UNO and 9 circularly polarized antennas. The circularly polarized antenna is designed using CST Microwave Studio which operate across 3-8.9GHz and the simulated and measured result shows great similarity. Arduino UNO is used to control the switching matrix together with stepper motor driver to ensure the antenna is switched on sequentially as well as ensuring it rotate in 50 steps with 7.2° angle. Then, MATLAB via a laptop will interface with the vector network analyzer and Arduino UNO during imaging process with realistic head phantom with simulated stroke and another without simulated stroke and as a result, 2 color gradient plots are generated. The difference in color shade between the two result shows that hemorrhagic stroke is detected.

Keywords: Stroke; Microwave Imaging System; Haemorrhagic

ABSTRAK

Sejak 2400 tahun yang lalu, penyakit strok masih terus berleluasa dalam semua lapisan masyarakat. Dengan kemajuan teknologi, mesin seperti tomografi berkomputer (CT) dan mesin pengimejan resonans magnetik (MRI) masih tidak dapat memberikan sebarang diagnosis bergerak. Oleh kerana saiz mesin yang besar dan juga menghasilkan radiasi berbahaya daripada mesin seperti CT, ambulans tidak lagi kondusif dan selamat untuk mengangkut pesakit jika mesin sebegitu dipasang di dalamnya. Kos operasi yang mahal dan tinggi bermaksud majoriti penduduk juga tidak mampu untuk akses rawatan sebegini. Oleh itu, di sinilah teknologi pengimejan gelombang mikro mampu membantu menyelesaikannya. Teknologi pengimejan gelombang mikro mampu menembusi tisu dan bahan dielektrik dan mesinnya selalunya adalah bersaiz sederhana dan mudah dibawa. Oleh itu, tujuan utama projek ini adalah untuk menganalisis sistem yang sedia ada, merancang dan membangunkan prototaip dan mengesahkan sistem. Sistem pengimejan gelombang mikro untuk pengesanan strok dibangunkan. Ia terdiri daripada platform berputar yang dikuasakan oleh Arduino UNO dan 9 antena berpolarisasi bulat. Antena berpolarisasi bulat direka bentuk dengan menggunakan CST Microwave Studio dan ia beroperasi di sepanjang frekuensi 3-8.9GHz dan hasil simulasi dan pengukuran menunjukkan banyak kesamaan antara mereka. Arduino UNO digunakan untuk mengawal matriks pensuisan bersama dengan pemacu motor pelangkah untuk memastikan antena dihidupkan secara berurutan dan diselaraskan antara satu sama lain. Sistem akan berputar 50 langkah dengan sudut 7.2 °. Kemudian, MATLAB melalui komputer riba akan bersambung dengan penganalisis rangkaian vektor dan Arduino UNO semasa proses pengimejan kepala phantom yang realistik dengan strok simulasi dan satu lagi tanpa strok simulasi dan akhirnya, 2 plot kecerunan warna akan dihasilkan. Perbezaan kecerahan warna antara kedua-dua plot ini menunjukkan bahawa strok pendarahan telah dikesan.

Kata Kunci: Strok; Sistem Pengimejan Gelombang Mikro; Pendarahan

INTRODUCTION

Stroke was first recognized over 2400 years ago by Hippocrates and is defined as a medical condition where there is interruption of blood supply to the brain causing the brain to be deprived of oxygen resulting in damage to the brain. In general, stroke is classified into ischemic stroke and haemorrhagic stroke. The difference between them is the cause whereby ischemic stroke is due to blood clot present in the arteries that supply blood to the brain while haemorrhagic stroke is due to rupturing of blood vessel which cause bleeding and increase in pressure to the brain.

Due to vast different in nature of these two strokes as shown in Figure 1, the treatment needed is also different and the important note here is that if the wrong treatment is administered to the patients, it will lead to more harm to the patients. Therefore, before providing any treatment, it is utmost important that doctors can identify the type of stoke the patient is suffering and then determine the best course of action in treating the patients. One wrong move and the patient will permanently harm for the rest of their life (National Institute of Neurological Disorders 2019).

A study conducted by Kooi et al. (2016) highlighted the severity of stroke among Malaysian and how stroke is impacting Malaysia in more ways than expected. Along with the study conducted by Aziz et al. (2016), it shows that there a still works to do to spread the awareness on the matter.

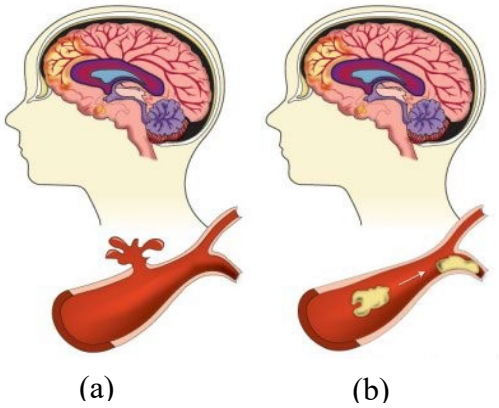

FIGURE 1: (a) is haemorrhagic stroke and (b) is ischemic stroke

Source: www.cdc.gov/stroke

One of the problems is the time taken for the patient to arrive to the hospital. From Table 1, it shows that the median arrival time taken via ambulance is 7.8 hours while for patients that arrive via own transport is 7.2 hours. However, the golden time window for patients to have an effective treatment is 4.5 hours and thus, every minute that goes by will have deadly consequences. The top contribution factor for late arrival are the ignorance and geographical location at 23% and 12.7% respectively.

TABLE 1: Median arrival time to stroke facility by different mode of transportation.

Source: Aziz et al. (2016)

Arrival Time	Via Ambulance		Via Own Transport		Other	
	n	%	n	%	n	%
<3 hours	1160	20.8	1576	28.6	18	32.1
>3 hours	2845	51.1	2083	37.8	16	28.6
>24 hours	1398	25.1	1367	24.8	8	14.3
Average Time of Arrival	7.8 hours		7.4 hours		4.6 hours	

In order to tackle this problem, there is a need for various innovation and creative solution in the area of prehospital and on the move diagnosis for treating stroke patients. It is this area that microwave imaging and diagnosis is capable to present a critical contribution. Over the past years, there are massive advancement for the utilizing of microwave imaging technology ranging from construction and even medical for breast cancer detection (A. T. Mobashsher & Abbosh 2014)

Microwave imaging technology provide an interesting prospect that it is capable of penetrating inside various object without doing any physical damage. For human body, we are consisted of a mixture of various dielectric material (Gabriel et al. 1996). This is unique because abnormalities that may present in our body will have different dielectric properties from healthy tissue. In the case of stroke, microwave imaging will be able to differentiate haemorrhagic stroke from ischemic stroke by detecting an unusual collection blood pool around the skull of the patients. The presence of blood pool in the skull will be eliminated the possibility of ischemic stroke.

Current stroke diagnosis imaging machines are often very bulky and huge which

result to immobility and thus inapplicable of portable solution. In addition to that, computed tomography (CT) scan uses high dose of radiation which is not suitable for long exposure and magnetic resonant imaging (MRI) scan is very complicated to operate and required highly skilled professional to handle (Fhager et al. 2018). In the meantime, for microwave imaging system, it is consisted of relatively small and portable component making it ideal for on-the-move diagnosis application and microwave also does not emits any hazards even under long exposure making it perfect to use as a diagnosis device installed in the ambulances. On-the-move diagnosis will help doctors and emergency respondents to provide preliminary aid and treatment to the patient before reaching the hospital.

In this work, the development of microwave imaging system for stroke detection get the inspiration of refurbishing an older microwave imaging system that serve a different purpose and converting it to be able to detect stroke. Therefore, this work has undergone three stages which are the investigation, development and validation stages. A realistic head phantom is developed based on a combination of recipes from researches conducted by Mohammed et al. (2014), Ahmed Toaha Mobashsher & Abbosh (2016) and Rokunuzzaman et al. (2019). Using that realistic head phantom, two set of condition which are one condition without stroke and another with stroke is simulated to test and validate the system which are a condition without stroke and another with stroke. The overall system is shown in Figure 2.

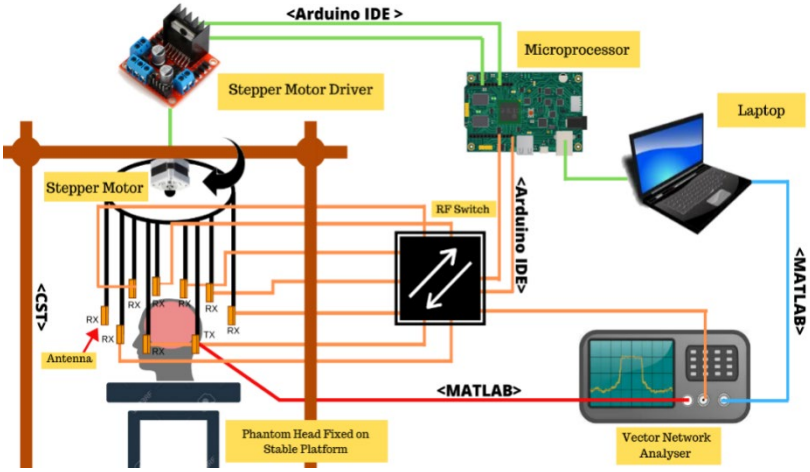

FIGURE 2: Overview of the microwave imaging system for stroke detection

METHODOLOGY

Figure 2 shows that this system includes nine circularly polarized antennas, perspex rotating platform, Arduino UNO, stepper motor, stepper motor driver, switching matrix, realistic head phantom, vector network analyser and laptop.

Antenna Design

During the process of antenna design, several reference and research paper are to understand the antenna used in microwave imaging system. The operating frequency and bandwidth of the antenna is very important for microwave imaging purpose.

Table 2 shows a comparison of operating frequency of antenna across different researchers. From there, it is inferred and concluded that the most desirable range should be between 1 GHz to 10 GHz. For this system, circularly polarized antenna is used, and the design is as shown in Figure 3. This type of antenna is very small and compact making it simple to be fabricated and low cost.

Table 2 : Investigation on the operating frequency

Research paper	Operating Frequency
Beadaa J. Mohammed et al. (2014)	1-4 GHz
Mobashsher, Abbosh, and Wang (2014)	1.1–3.4 GHz
Bakar et al. (2012)	3.1-10.6 GHz

The antennas have several unique designs that is worth to be discussed. One of the most noticeable aspect of this antenna is the crescent like shape printed on the front (Figure 3) and then a circular slot etched out at the back of the antenna (Figure 4). The crescent shape in the front provide the circular polarization characteristic to the antenna while the circular slot at the back will improve the bandwidth of the antenna. Thus, these few features result in an interesting and unique look while achieving all the working intent purpose. This antenna is fabricated on an epoxy resin (FR4) that had the relative permittivity of 4.5 and

dielectric loss of 0.02 as well as the dimension of the antenna are 30 x 30 x 1.6 mm.

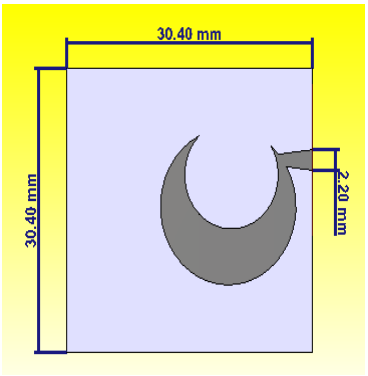

FIGURE 3: Front view of the circularly polarized antenna

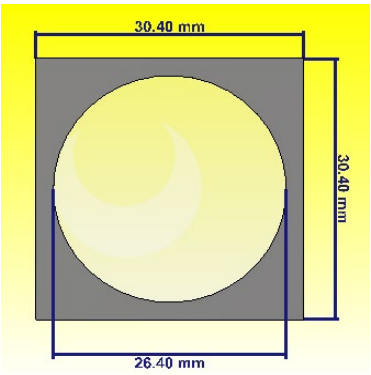

FIGURE 4: Front view of the circularly polarized antenna

Rotating platform design

The rotating platform is the bridge between the imaging process and the data analysis process. The rotating platform acts as the house for all nine antennas as well as other component such the stepper motor, stepper motor driver, Arduino UNO and switching matrix. Figure 5 show the flowchart of the programming sequence and logic of the system operation.

From the flowchart, the step angle is 7.2° and this is because the desired number of step for the imaging process is 50 which is the compromise sweet spot between the time take for one full circle rotation and amount of data needed to make meaningful analysis. The loop of increasing a step of 7.2° and capturing back scatter signal will be terminated after 50 steps or 360° is achieved. For the process of imaging and generating a colour contour graph, it is estimated to take around 8-10 minutes and it may be faster depending on the type of laptop used with new and faster processor making it faster.

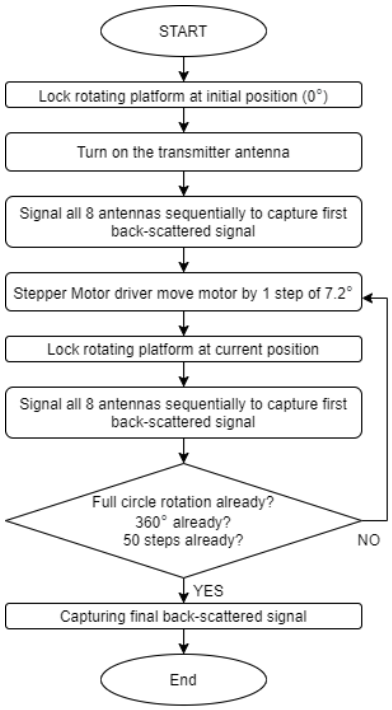

FIGURE 5: Flowchart of motor and antenna switching sequence

Realistic Head Phantom Fabrication

For the fabrication of a head phantom, inspirations of the recipe are taken from research of Mobashsher & Abbosh (2014), Mohammed et al. (2014), and Rokunuzzaman et al. (2019). Five tissue has been fabricated which are dura, cerebral spinal fluid, grey matter, white matter and blood.

The fabricated head phantom has undergone testing using a dielectric probe. This probe test is very popular and easy to execute because it is one of the non-destructive tests that does not affect the measured substance. The probe can measure the phantom in terms of relative permittivity and conductivity. The measured result will then be compared to those measured in Mobashsher & Abbosh (2014). Comparison and analysis will be conducted to determine the quality of the phantom fabricated. The general procedure for the fabrication of different layers of brain replicated are as shown in Figure 6. Table 3 is the total recipe used for fabricating the head phantom in this project. Once fabrication is completed, the sequence of how the layers of tissues is inserted in the skull model is also crucial and Figure 7 shows the layering sequence for the phantom.

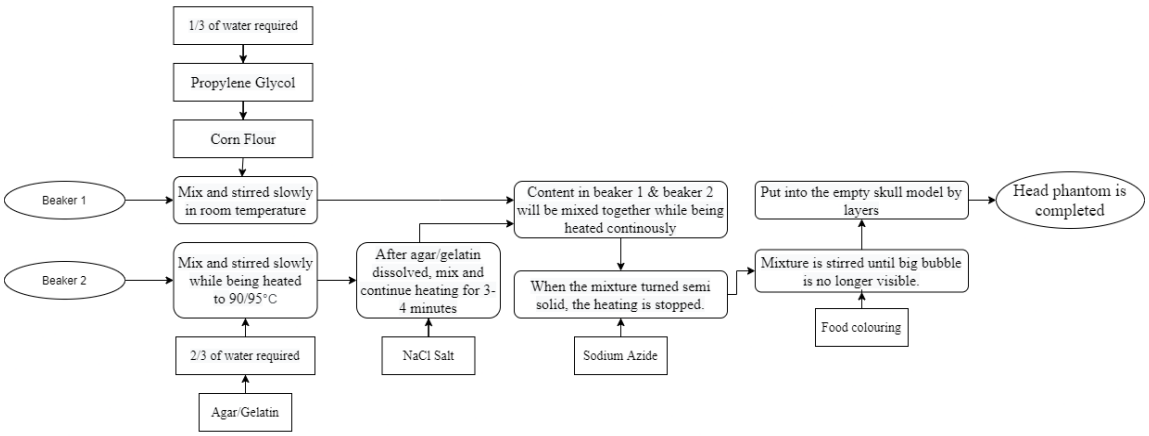

FIGURE 6: Flowchart of head phantom fabrication

Table 3: Recipe for head phantom fabrication

Items	Quantity (g)					Purpose
	Blood	CSF	Dura	White Matter	Grey Matter	
Water	81.97	167.4	144.75	141.3	241.9.5	Main source of permitivity
Corn Flour	2.74	4.06	48.26	53.7	49.77	Relative permittivity control.
Agar	2.75	22.48	1.96	0	3.12	Thickener
Gelatin	0	0	0	2.82	0	Thickener
Sodium Azide	0.36	0.74	0.72	0.7	1.05	Preservative.
Propylene Glycol	0.91	2.98	3.86	1.42	2.76	Stabilizing agent
NaCl Salt	1.28	2.24	0.48	0	1.38	Preservative.

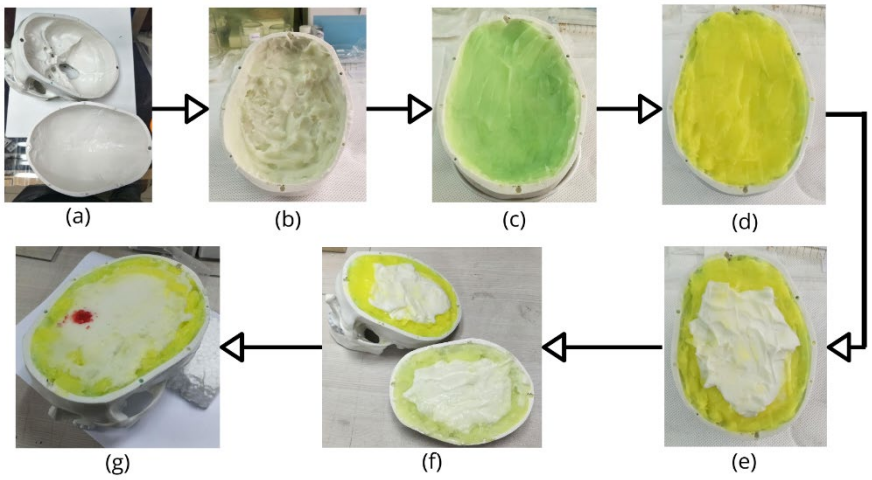

FIGURE 7: Sequence of layering of fabricated tissue where (a) is empty skull model, (b) is the dura layer,(c) is the CSF layer,(d) grey matter,(e)white matter,(f) filled skull model and (g) filled skull model with simulated stroke

Testing and Validation

In testing and validation of the system, three sets of imaging data has been executed. First set of imaging data is the imaging without any object under the rotating platform and this can determine the imaging area covered by the system. Second set of imaging data is the imaging of head phantom without simulated stroke and this part determines location of the head phantom under the rotating platform. Finally, the third imaging set is the imaging of head phantom with simulated stroke and the data obtained is to be compared to the data of first and second set to obtain the exact location of the bleeding occur.

The imaging data collected then be process via MATLAB software. Two colour contour graphs has been generated where one is for head phantom without simulated stroke and the other for head phantom with simulated stroke. Both graphs are compared with each other to determine whether the bleeding is captured. The graph for the head phantom with simulated stroke is expected to have more shades of yellow and red as the presence of extra blood tissue will cause the back-scattered signal captured to be weaker compared to the phantom without simulated stroke.

RESULT & DISCUSSION

Antenna Analysis

Several parameters are being use as the guide to analysis the antenna performance. The simulation is done using the CST Microwave Studio 2019.

One of those parameters is the reflection coefficient or S11 parameter. In general, the S11 parameter is used to determine the operating frequency of the antenna. As mentioned before, the preferred operating frequency for any microwave imaging system should be between 1 GHz to 10 GHz. It is determine based on the range of frequency that the antenna operate when it falls below -10 dB. Using -10 dB means that only 10% of the input power being reflected of the antenna while the remaining is delivered completely.

Figure 6 shows the simulated and measured result for S11 parameter. From there, we can see that despite having some difference between both values which may be due to equipment tolerance and non-ideal environment , it can be concluded that both result display a similar trend and general pattern and thus, it is good enough to infer that the antenna operated at the frequency range of 3 GHz till 8.9 GHz with the bandwidth of 5.9 GHz.

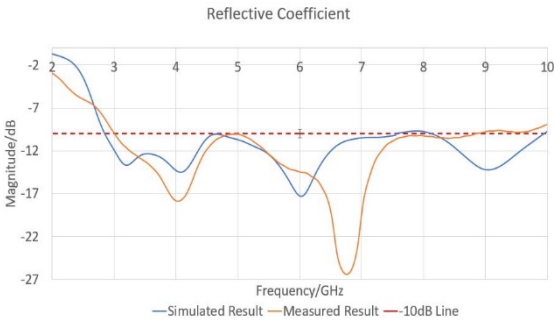

FIGURE 8: Reflective Coefficient (S11)

Next is the gain of the antenna. From CST Microwave Studio 2019, it is capable of simulating gain and realized gain. What will be taking into consideration here is the realized gain as it provides a clearer picture of the performance of the antenna. Realized gain is gain calculation that take losses due to reflection and losses due to structure of antenna into consideration.

With that said, Figure 7 is the result of the simulated and measured gain. Similar situation here is that the value has a general similar trend with minor difference which may be due to equipment tolerance and non-ideal environment. However, with a similar trend begin observed into both values, it is concluded that the gain of the antenna operating between 3 GHz and 8.9 GHz is in the range of 1.1 dB to 13 dB in general.

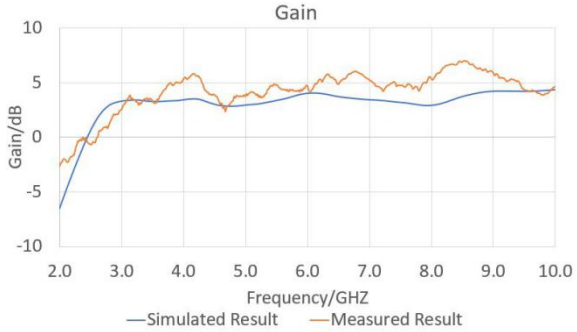

FIGURE 9: Antenna Gain

Following the list, the radiation pattern is examined. The radiation pattern at the operating frequency of 3.1 GHz, 4.1 GHz, and 6.0 GHz is observed in 2D and 3D because those frequency are noted to be peak during the S11 parameter graph and thus the making it, the probable point of interest for radiation pattern analysis.

Figure 9 show the simulated 2D radiation pattern and Figure 10 shows the 3D radiation pattern of the antenna. The red color is the indicator of maximum power and field in the radiation pattern.

Thus, observing Figure 10, the presence of red show that there ample of red shade throughout the field at difference frequency. From there, it is can be concluded that the radiation pattern of the

antenna is stable and strong throughout the operating frequency.

3.1GHz

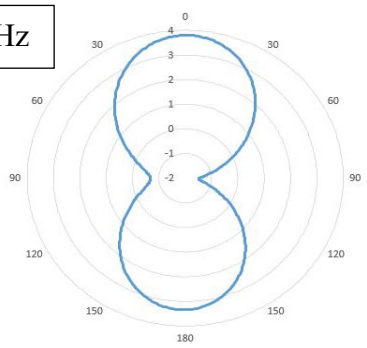

4.1GHz

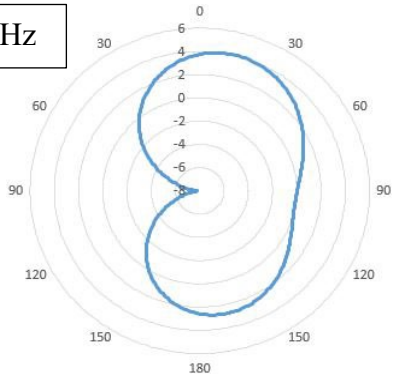

6.0GHz

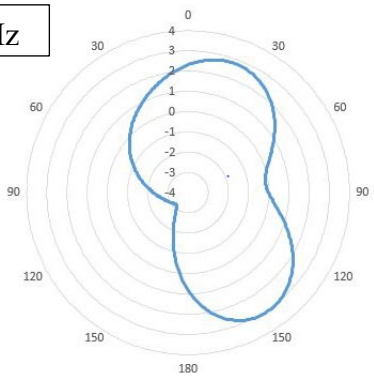

FIGURE 10 2D radiation pattern

3.1GHz

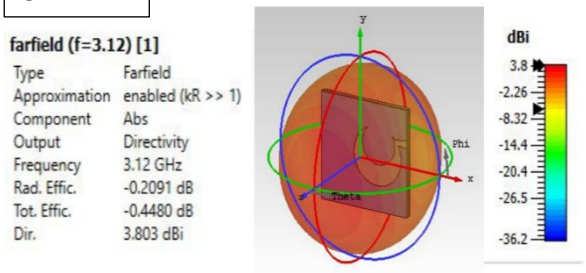

4.1GHz

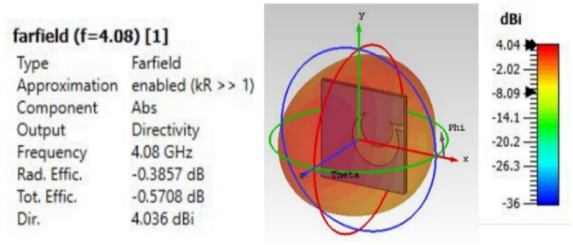

6.0GHz

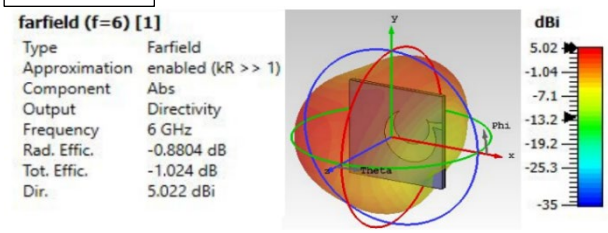

FIGURE 11 3D radiation pattern

Testing of Fabricated Head Phantom

Six layers tissues were fabricated which are the dura, CSF, white matter, grey matter and blood. Figure 12 and Figure 13 are the final product after all six layers of fabricated tissue is being inserted. Each tissue has been tested under KEYSIGHT 85070E dielectric probe operated by 805070 dielectric software together with vector network analyzer PNA-L N5232A. The dielectric probe can measure relative permittivity and conductivity in the frequency range between 0.5 GHz to 5 GHz. Before the probe is used to measure the fabricated materials, it is first calibrated by measuring sterile water. From there, the probe is inserted vertically and slightly pressed on the surface of the fabricated materials to ensure that there is no air gap in between those two. Two sets of data has been recorded, and the mean result is tabulated and presented in graph.

FIGURE 12: Head phantom without simulated stroke

FIGURE 13: Head phantom with simulated stroke.

The graph in Figure 14 is for the relative permittivity result for all the layers. This result obtained in the graph is then compared to those measured in the research paper by Mobashsher & Abbosh (2014) and it proves that the fabricated phantom exhibit similar relative permittivity properties with those done in Mobashsher & Abbosh (2014).

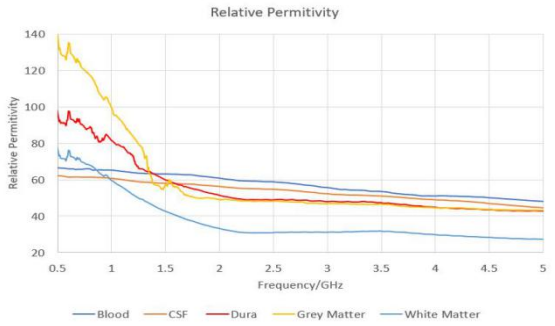

FIGURE 14: Relative Permitivity

The graph in Figure 15 is for the conductivity result for all the layers. This result obtained in the graph is also then compared to those measured in the research paper by Mobashsher & Abbosh (2014) and again prove great agreement in result between those two.

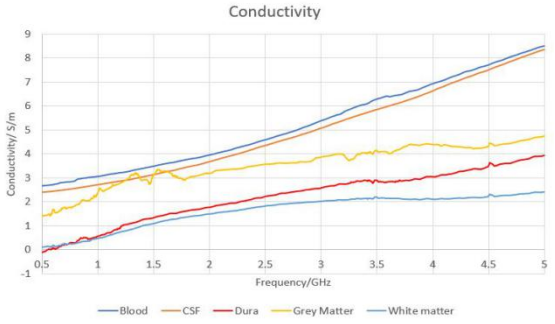

FIGURE 15: Conductivity

System validation

As mentioned before, three sets of imaging process has been taken. During the placement of head phantom, it is a must to ensure that the location doesn't change by putting marking at the placed position. This is to ensure that when comparing data in finding the location of phantom head, there won't be any human caused arrived.

After processing the first and second set of imaging data where simulated stroke is absent in both set of imaging process, color contour graph in Figure 16 is obtained. It is observed that the whole graph is covered in blue which indicated the absence of simulated stroke is validated.

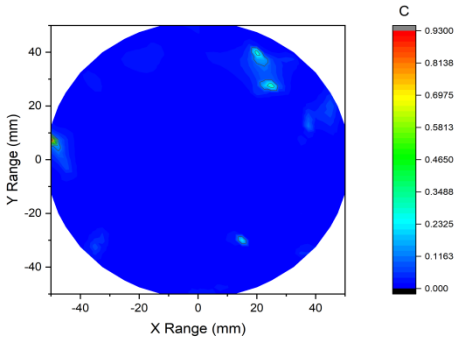

FIGURE 16: Color contour graph for head phantom without simualted stroke

From there the third set of imaging where simulated stroke is presence, the color contour graph in Figure 17 is obtained. From here, when comparison is made with the graph in Figure 16, we can see that at the circled position, there more shades of yellow and red presence in the graph. At the lower left side of the graph, a bright red spot that indicate weak signal is observed and this spot correlated with the location of simulated stroke.

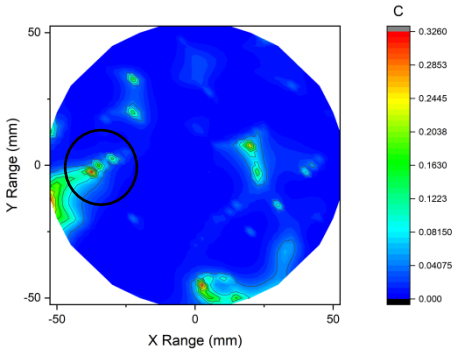

FIGURE 17: Color contour graph for head phantom with simualted stroke

A weak signal is captured because due to the presence of simulated stroke at that region means that more material for absorption of signal is also presence. Thus, that extra materials help in absorbing more signal resulting in weaker back scattering signal at that region compared to other part of the head phantom.

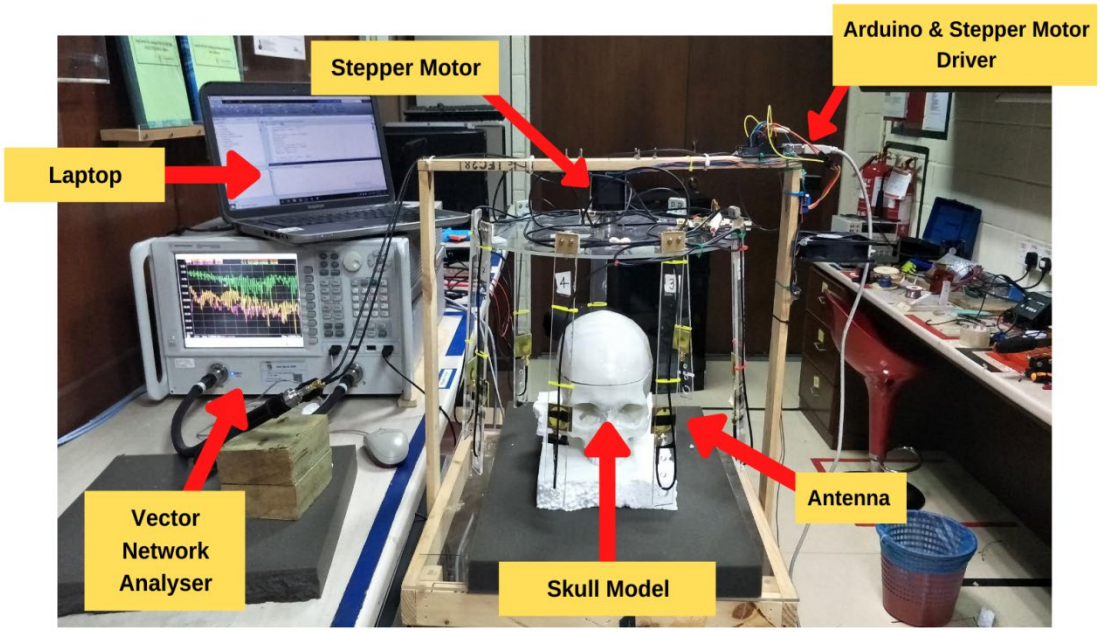

FIGURE 18 : System setup during validation

CONCLUSION

In conclusion, a microwave imaging system for stroke detection is developed. The system is consisted of nine circularly polarized antenna with the operating frequency of 3 GHz and 8.9 GHz and bandwidth of 5.9 GHz, achieving stable and strong radiation pattern. The rotating platform developed can operate 50 steps in one full circle rotation with 7.2° per step which is entirely powered by a stepper motor and managed by an Arduino UNO. A realistic head phantom for simulating stroke condition is also successfully fabricated and tested. In the system validation process, the color gradient plot for both set of data whereby one is collected without simulated stroke and another with simulated stroke is obtained. The location of the simulated stroke was determined to be at the lower left side of the graph which correlated to the location of simulated stroke in head phantom. The capturing of a brighter and yellow color for the head phantom with simulated stroke validate that the system can detect hemorrhagic stroke. To be able to capture this distinct and unique characteristic of hemorrhagic stroke, it will help the emergency respondent in differentiating hemorrhagic stroke from other type of stroke and increase the effectiveness of the proceeding treatment.

ACKNOWLEDGEMENT

This work is supported by Universiti Kebangsaan Malaysia under the grant code of GUP-2019-005.

REFERENCES

Aziz, Z. A., Sidek, N. N., Kamarudin, M. K., Baharum, N., Muneer, A., Hamid, A., Lutfi, A., et al. 2016. Annual Report of the Malaysian.

Bakar, A. A., Ireland, D., Abbosh, A. & Wang, Y. 2012. Experimental assessment of microwave diagnostic tool for ultra-wideband breast cancer detection. *Progress In Electromagnetics Research M* 23(July 2018): 109–121. doi:10.2528/PIERM11122102

Fhager, A., Candefjord, S. & Elam, M. 2018. Microwave Diagnostics Ahead (April): 78–90.

Gabriel, S., Lau, R. W. & Gabriel, C. 1996. The dielectric properties of biological tissues: II. Measurements in the frequency range 10 Hz to 20 GHz. *Physics in Medicine and Biology* 41(11): 2251–2269. doi:10.1088/0031-9155/41/11/002

Kooi, C. W., Peng, H. C., Aziz, Z. A. & Looi, I. 2016. A review of stroke research in Malaysia from 2000 – 2014. *Medical Journal of Malaysia* 71(June): 58–69.

Mobashsher, A. T. & Abbosh, A. M. 2014. Three-dimensional human head phantom with realistic electrical properties and anatomy. *IEEE Antennas and Wireless Propagation Letters* 13: 1401–1404. doi:10.1109/LAWP.2014.2340409

Mobashsher, Ahmed Toaha & Abbosh, A. M. 2016. Performance of directional and omnidirectional antennas in wideband head imaging. *IEEE Antennas and Wireless Propagation Letters* 15(March): 1618–1621.

doi:10.1109/LAWP.2016.2519527

Mohammed, B. J., Abbosh, A. M., Mustafa, S. & Ireland, D. 2014. Microwave system for head imaging. *IEEE Transactions on Instrumentation and Measurement* 63(1): 117–123. doi:10.1109/TIM.2013.2277562

National Institute of Neurological Disorders. 2019. Stroke : Hope Through Research 1–50.

Rokunuzzaman, M., Ahmed, A., Baum, T. C. & Rowe, W. S. T. 2019. Compact 3-D Antenna for Medical Diagnosis of the Human Head. *IEEE Transactions on Antennas and Propagation* 67(8): 5093–5103. doi:10.1109/tap.2019.2908066